

Analysis of a simple method for the reduction of phonon peak broadening in surface Brillouin Light Scattering

Christian Gigault and John R. Dutcher

We present an investigation of the effect of the collecting lens aperture on the line shape of phonon peaks observed in surface Brillouin light scattering (SBLs) from surfaces of opaque materials and transparent thin films. In general, the broadening that is due to the aperture is asymmetric and can be as large as 60% of the peak frequency shift in the case of a $f/1.4$ aperture with an angle of incidence $\theta_i = 30^\circ$. We calculated SBLs spectra accounting for the spread in scattering wave vectors across the collecting lens aperture, the polarization and angular dependence of the scattering, and the spectrometer instrumental function. By performing a detailed comparison between measured and calculated SBLs spectra for Si(001), we identified a set of simple rules for the placement of a rectangular slit in the collecting lens aperture to reduce the effects of aperture broadening. By use of a slit, the peak linewidths can be reduced substantially, without reducing the peak heights significantly, while eliminating false shifts in the measured frequency values. © 1998 Optical Society of America

OCIS codes: 290.0290, 290.5830, 300.6330, 310.0310.

1. Introduction

Brillouin light scattering (BLS) is a powerful, nondestructive technique for the measurement of the elastic properties, acoustic attenuation, structural relaxation, and phase transitions of bulk transparent materials.¹⁻³ These measurements involve volume scattering of light from long-wavelength, bulk phonons within the material. Because of recent advances in BLS instrumentation that are attributed to Sandercock,³ BLS is now a powerful tool for the study of a wide variety of opaque bulk materials, such as metals and semiconductors, as well as opaque and transparent thin films. For opaque materials, the scattering volume is essentially a sheet near and parallel to the sample surface, with a thickness that is comparable to the optical skin depth δ_{opt} of the material (~ 15 nm for metals). These same restrictions on the scattering volume also apply to BLS studies of thin films, with thicknesses that are much smaller than the wavelength of light. Because of the sheet-like nature of the scattering volume, which gives rise to surface Brillouin light scattering (SBLs), only the

wave-vector components that are parallel to the sample surface are conserved in the scattering process.⁴ If the scattered light wave vector lies in the plane of incidence, the phonon wave vector $\mathbf{Q}_{\parallel} = \pm(k_{\parallel}^s - k_{\parallel}^i)$, where k_{\parallel}^s and k_{\parallel}^i are components of the scattered and incident wave vectors parallel to the sample surface, and the plus and minus signs correspond to anti-Stokes and Stokes-scattering events, respectively.

Because the lens that is used to collect the scattered light accepts scattered wave vectors \mathbf{k}^s in a range of directions, there is a corresponding spread in the magnitude and direction of the phonon wave vector \mathbf{Q}_{\parallel} . This causes a corresponding frequency broadening of the phonon peak in the measured BLS spectra.

For BLS from bulk transparent materials, broadening of the Brillouin peaks that is due to the nonzero collecting lens aperture has been studied previously.^{5,6} The aperture broadening is a function of the scattering angle γ , which is the angle between incident and scattered light wave vectors. The magnitude of the phonon wave vector Q probed in this case is given by $Q = 2k^i \sin(\gamma/2)$. For the $\gamma = 90^\circ$ scattering geometry, the spread in Q that is due to aperture broadening has its maximum value. For $\gamma = 0$ (forward-scattering geometry) and for $\gamma = 180^\circ$ (back-scattering geometry), the spread in Q that is due to aperture broadening is very small, even for apertures as large as $f/1.4$. This results in a broadening that is smaller than the spectrometer's instrumental linewidth, which is of the order of 1 GHz.

For SBLs measurements, the effects of aperture

The authors are with the Department of Physics and the Guelph-Waterloo Program for Graduate Work in Physics, University of Guelph, Guelph, Ontario N1G 2W1, Canada.

Received 3 June 1997; revised manuscript received 5 January 1998.

0003-6935/98/153318-06\$15.00/0

© 1998 Optical Society of America

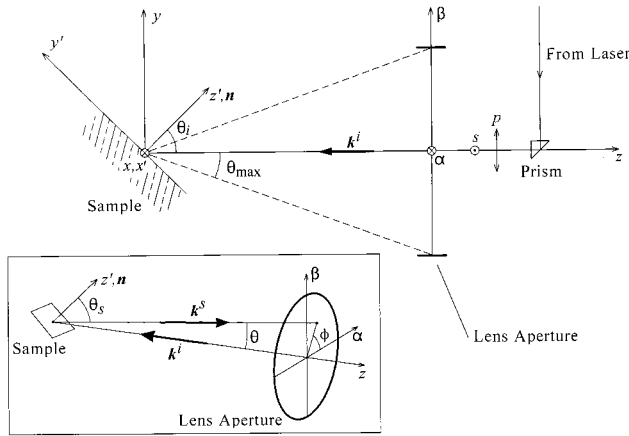


Fig. 1. Surface Brillouin light scattering geometry. p and s refer to the polarization of the light. The plane of the figure is the plane of incidence. The inset shows the scattered wave vector \mathbf{k}^s , which is not necessarily in the plane of incidence. The scattered angle θ_s is measured between \mathbf{k}^s and the sample normal \mathbf{n} .

broadening can be much larger than for BLS from bulk transparent materials. Recently, a rectangular slit has been used to reduce aperture broadening in SBL experiments.⁷⁻¹⁰ In particular, the use of a slit was crucial for the careful comparison of experimental and theoretical SBL spectra for surface gratings on Si(001).^{8,11} It is also necessary for the accurate measurement of Brillouin peak linewidths and for measurements of crystalline anisotropy, as discussed below. In this paper we present a detailed analysis of the role of the slit in the reduction of peak broadening in SBL experiments. First we present a calculation of the phonon peak broadening in SBL experiments that is due to the nonzero aperture of the collecting lens for the common 180° backscattering geometry, accounting for the direction of the light polarization and the angular dependence of the scattering cross section for surface scattering and allowing the scattered light wave vector to lie out of the plane of incidence. By calculating contour plots of Q_{\parallel} across the collecting lens aperture, we identified a set of simple rules for the placement of the slit in the aperture. The calculation results are compared with SBL measurements performed on a Si(001) wafer with a tandem six-pass Fabry-Perot interferometer, with and without the use of a slit. From this comparison, we show that, with proper placement, the use of a slit in the scattered light is an effective method for reducing the aperture broadening without reducing the signal-to-noise ratio significantly and for eliminating false shifts in the measured frequency values.

2. Description of the Calculation

First we describe the backscattering geometry used in the SBL experiment, as illustrated in Fig. 1. For brevity, we assume that the index of refraction of air is unity and do not include it explicitly in our treatment. Laser light of vacuum wavelength λ is directed onto a lens that focuses the light onto the

sample surface. The angle between the incident light and the sample normal \mathbf{n} is θ_i (the angle of incidence) and the incident light wave vector is \mathbf{k}^i , where $k^i = 2\pi/\lambda$. The scattered light is collected by the same lens. Because the lens aperture has a nonzero size, there is a spread in the direction of the collected scattered light wave vector \mathbf{k}^s . The total solid angle Ω subtended by the circular aperture of the lens is determined by the maximum acceptance angle θ_{\max} that is specified by the f -number ($f/\#$) of the lens: $\theta_{\max} = \tan^{-1}[1/(2f/\#)]$; e.g., $\theta_{\max} = 19.7^\circ$ for $f/1.4$.

The plane of the lens aperture is defined by the α and β axes. A set of axes x', y', z' rotated about the x axis by an angle θ_i is defined, such that the sample surface is the x', y' plane. The plane of incidence is the $y'-z'$ plane. In the case of pure 180° backscattering (i.e., for an infinitesimal lens aperture diameter), the magnitude of the phonon wave vector probed by SBL with this geometry is simply $Q_{\parallel} = 2k^i \sin \theta_i = (4\pi/\lambda) \sin \theta_i$. The phonon wave vector \mathbf{Q}_{\parallel} , which lies in the $x'-y'$ plane, depends on θ_i through the orientation of the incident wave vector \mathbf{k}^i and also depends on the orientation of the scattered wave vector \mathbf{k}^s which itself is characterized by the spherical coordinate variables θ and ϕ , with θ measured with respect to the z axis and ϕ measured with respect to the x axis in the $x-y$ plane (Fig. 1). The phonon wave vector is given by $\mathbf{Q}_{\parallel} = \pm(\mathbf{k}_{\parallel}^s - \mathbf{k}_{\parallel}^i)$, where the parallel component of a vector \mathbf{A} is defined as $\mathbf{A}_{\parallel} \equiv \mathbf{A} - (\mathbf{A} \cdot \mathbf{n})\mathbf{n}$.

For the calculation of light scattering from the phonon modes of a sample, it is convenient to express the incident, scattered, and phonon wave vectors in the sample reference frame x', y', z' :

$$\mathbf{k}_{\parallel}^i = k^i \sin \theta_i \mathbf{j}', \quad (1)$$

$$\mathbf{k}_{\parallel}^s = k_x^s \mathbf{i}' + (\cos \theta_i k_y^s - \sin \theta_i k_z^s) \mathbf{j}', \quad (2)$$

$$\mathbf{Q}_{\parallel} = \pm k^i \{ \sin \theta \cos \phi \mathbf{i}' + [\cos \theta_i \sin \theta \sin \phi - \sin \theta_i \times (1 + \cos \theta)] \mathbf{j}' \}, \quad (3)$$

where $\mathbf{i}', \mathbf{j}', \mathbf{k}'$ are unit vectors along the $x', y',$ and z' axes, respectively. To obtain the expression for \mathbf{Q}_{\parallel} , we expressed $k_x^s, k_y^s,$ and k_z^s in terms of θ and ϕ , which are measured with respect to the laboratory frame $x, y, z,$ and we used $|\mathbf{k}^s| \approx |\mathbf{k}^i|$ (because the phonon frequency is much smaller than the light frequency). For the case of an aperture with an infinitesimal diameter, we recover $Q_{\parallel} = 2k^i \sin \theta_i$ for pure 180° backscattering.

To calculate the shape of the broadened peak, one has to first calculate the scattered light intensity I_s corresponding to specific values of θ_i and θ_s , the latter being measured between \mathbf{k}^s and \mathbf{n} , with $\cos \theta_s = (\mathbf{k}^s \cdot \mathbf{n})/k^s$. A set of expressions for the cross section of the scattering of light by a small static ripple on the surface have been given by Agarwal¹² for incident and scattered light of general orientation and polarization. The treatment also applies to light scattering from surface excitations with frequencies much smaller than the incident light frequency, such as the

Rayleigh mode probed by SBLs.¹³ The incident light polarization can be decomposed into p -polarized and s -polarized components. Similarly, the scattered light polarization can be decomposed into parallel and perpendicular components with respect to the plane formed by \mathbf{k}^s and \mathbf{n} . Because the amplitude of the Rayleigh mode has a $1/Q_{\parallel}$ dependence,¹³ the angular dependence $F(\theta_i, \theta, \phi)$ of the Rayleigh mode differential cross section $d\sigma/d\Omega$ for the different polarization cases is as follows:

$$\begin{aligned} \frac{d\sigma}{d\Omega} \propto F(\theta_i, \theta, \phi) \equiv & \frac{\cos^2 \psi \cos^2 \theta_s \cos \theta_i}{(Q_{\parallel}/k^i)} \left| \frac{\epsilon - 1}{[\cos \theta_s + (\epsilon - \sin^2 \theta_s)^{1/2}][\cos \theta_i + (\epsilon - \sin^2 \theta_i)^{1/2}]} \right|^2, s \rightarrow s \\ & \frac{\sin^2 \psi \cos^2 \theta_s \cos \theta_i}{(Q_{\parallel}/k^i)} \left| \frac{(\epsilon - 1)(\epsilon - \sin^2 \theta_s)^{1/2}}{[\epsilon \cos \theta_s + (\epsilon - \sin^2 \theta_s)^{1/2}][\cos \theta_i + (\epsilon - \sin^2 \theta_i)^{1/2}]} \right|^2, s \rightarrow p \\ & \frac{\sin^2 \psi \cos^2 \theta_s \cos \theta_i}{(Q_{\parallel}/k^i)} \left| \frac{(\epsilon - 1)(\epsilon - \sin^2 \theta_i)^{1/2}}{[\cos \theta_s + (\epsilon - \sin^2 \theta_s)^{1/2}][\epsilon \cos \theta_i + (\epsilon - \sin^2 \theta_i)^{1/2}]} \right|^2, p \rightarrow s \\ & \frac{\cos^2 \theta_s \cos \theta_i}{(Q_{\parallel}/k^i)} \left| \frac{(\epsilon - 1)[\cos \psi (\epsilon - \sin^2 \theta_s)^{1/2} (\epsilon - \sin^2 \theta_i)^{1/2} - \epsilon \sin \theta_i \sin \theta_s]}{[\epsilon \cos \theta_s + (\epsilon - \sin^2 \theta_s)^{1/2}][\epsilon \cos \theta_i + (\epsilon - \sin^2 \theta_i)^{1/2}]} \right|^2, p \rightarrow p \end{aligned} \quad (4)$$

where ϵ is the complex dielectric constant of the sample and the angle ψ is measured between the vectors \mathbf{k}_{\parallel}^i and \mathbf{k}_{\parallel}^s in the sample surface plane x', y' , obtained from the dot product of \mathbf{k}_{\parallel}^i and \mathbf{k}_{\parallel}^s .

For the calculation of SBLs line shapes presented below, in general it is necessary to account for the effects of anisotropy, the phonon intrinsic linewidth, and the instrumental linewidth of the Fabry–Perot interferometer. For the present analysis, the material was taken to be isotropic: For many materials, including silicon, the effect of anisotropy on the line shape is much smaller than aperture effects. In addition, the natural linewidth of the Rayleigh phonon was taken to be much smaller than the BLS spectrometer instrumental linewidth, i.e., the natural phonon line shape was taken to be a Dirac delta function (it is straightforward to account for a non-zero natural linewidth at this stage).

The collected intensity spectrum I_c is given by the sum over the solid angle subtended by the lens aperture:

$$I_c(\omega) = \int_0^{\theta_{\max}} \sin \theta d\theta \int_0^{2\pi} d\phi I_s[\mathbf{Q}_{\parallel}(\theta, \phi, \theta_i), \omega], \quad (5)$$

in which θ_{\max} is as defined above, and the quantity I_s has the form

$$I_s[\mathbf{Q}_{\parallel}(\theta, \phi, \theta_i), \omega] \propto F(\theta, \phi, \theta_i) \times \delta(\omega - \mathbf{Q}_{\parallel} v_R), \quad (6)$$

where F is given by Eq. (4), v_R is the (isotropic) velocity of the Rayleigh mode, and Q_{\parallel} is the magnitude of the phonon wave vector.

To compare calculated spectra with measured spec-

tra, it is necessary to convolve I_c as given by Eq. (5) with the Fabry–Perot interferometer resolution function, which is approximated well by a Lorentzian curve raised to the power p , where p represents the number of passes through the Fabry–Perot interferometer.

3. Calculation Results and Discussion

To a good approximation, the magnitude of all the scattered wave vectors \mathbf{k}^s is constant. The locus of their end points defines a sphere centered at the or-

igin of the x, y, z frame, and the collecting aperture accepts a portion of that sphere. Each direction of the vector \mathbf{k}^s is associated with a phonon wave vector \mathbf{Q}_{\parallel} given by Eq. (3), and therefore the curves of constant $|\mathbf{Q}_{\parallel}| = Q_{\parallel}$ lie on the sphere defined by the scattered wave vectors. One can obtain a contour plot of Q_{\parallel} as a function of the position in the plane of the aperture by projecting the curves of constant Q_{\parallel} onto the plane of the aperture. A scattered wave vector \mathbf{k}^s can be located in this plane by use of the dimensionless coordinates α and β (Fig. 1), defined, for the purposes of illustration, by the simple prescription $\alpha = \sin \theta \cos \phi$ and $\beta = \sin \theta \sin \phi$, which is accurate to within 4% for an aperture of $f/1.4$. The lens aperture is therefore a circle in (α, β) coordinates with a radius equal to $\sin \theta_{\max}$. In Figs. 2(a) and 2(b) we present contour plots of Q_{\parallel} (solid lines) as a function of the aperture coordinates (α, β) for $\theta_i = 30^\circ$ and $\theta_i = 70^\circ$, respectively. The circles shown in the figures delimit the areas accepted by $f/1.4$ and $f/2$ lenses. The two cross-hatched rectangular areas correspond to the position and shape of slits used in SBLs experiments described below in Section 4. In addition, the shadow of the right-angle prism and its supporting rod (Fig. 1) is shown as a cross-hatched area in Figs. 2(a) and 2(b). The points **a**, **b**, **c**, and **d**, which lie within the slits, refer to the insets in which the orientations of the corresponding phonon wave vector \mathbf{Q}_{\parallel} are illustrated with respect to the sample surface plane x', y' . It is worthwhile to note that this spread in the direction of \mathbf{Q}_{\parallel} can cause errors in the measurement of crystalline anisotropy by use of SBLs. The total range of values of Q_{\parallel} accepted by the $f/1.4$ lens is $\pm 30\%$ for $\theta_i = 30^\circ$ and $+3\%$ and -9% for $\theta_i = 70^\circ$ (this

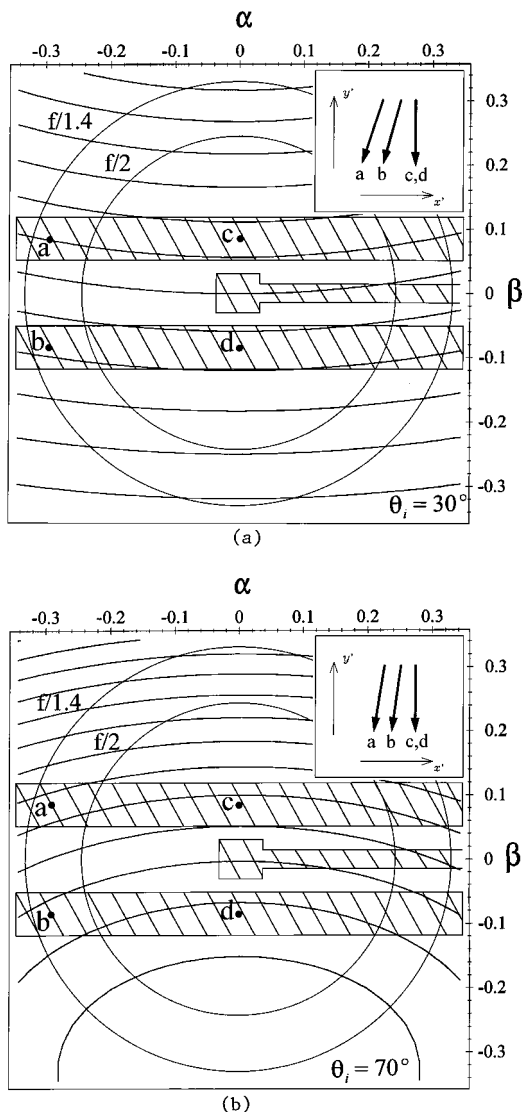


Fig. 2. (a) Contour plot of the magnitude of Q_{\parallel} for $\theta_i = 30^\circ$. The circles represent lens apertures and the inset shows the orientation of the phonon wave vector with respect to the sample surface plane x', y' , corresponding to points **a**, **b**, **c**, and **d**. ΔQ_{\parallel} between curves is $0.05 \times k^i$. The cross-hatched areas are described in the text. (b) Same as in (a) but for $\theta_i = 70^\circ$ and ΔQ_{\parallel} between curves is $0.02 \times k^i$.

corresponds to $\beta = \pm 0.336$ with $\alpha = 0$. This range of Q_{\parallel} corresponds for $\theta_i = 30^\circ$ to a total broadening of 60% of the phonon peak in a SBLs spectrum.

The peak broadening that is due to the nonzero diameter of the collecting lens aperture can be reduced simply by stopping down the aperture of the lens, i.e., reducing the diameter of the aperture symmetrically around its center. However, this scheme increases the relative amount of the aperture blocked by the right-angle prism and its supporting rod. Ideally one should use an aperture that can be adjusted to follow the curves of constant Q_{\parallel} as the angle of incidence is varied [Figs. 2(a) and 2(b)]. Unfortunately, this is not easy to do if one requires that measurements be performed for different values of θ_i .

However, one can obtain a good approximation to a constant Q_{\parallel} aperture by using a rectangular slit that accepts only a portion of the scattered beam in which the value of Q_{\parallel} is relatively constant. There are several rules that should be followed when such a slit is used in SBLs measurements. It is best to place the slit after the collecting lens, where the beam is collimated and of relatively large diameter. The long dimension of the slit should be along the α direction and the optimal position of the slit is in the negative β region, because for negative β and all angles of incidence the curves of constant Q_{\parallel} are more widely spaced [Figs. 2(a) and 2(b)]. Also, the slit should be placed close to the center of the aperture to maximize the amount of collected light, such that it is not in the shadow of the small prism and its mounting rod [Figs. 1, 2(a), and 2(b)]. A rectangular slit, as opposed to an aperture following the shape of the constant Q_{\parallel} contour curves, is sufficient because the goal is to only reduce the aperture broadening to a value smaller than the BLS spectrometer instrumental linewidth.

There is a shift between the measured peak positions in the slit spectra and the ideal position (i.e., for an infinitesimal lens aperture diameter) because of the difference in the average value of Q_{\parallel} produced by the offset of the slit from the center of the aperture. The value of Q_{\parallel} in the center of the slit is given by

$$Q_{\parallel} = k^i |\sin \theta_i + \sin(\theta_i - \delta)|, \quad (7)$$

where the angle δ is related, for example, to the displacement $\beta = \beta_{\text{slit}}$ of the center of the slit from the z axis (see Fig. 1): $\delta = \sin^{-1}(\beta_{\text{slit}})$.

4. Experimental Results and Discussion

In Figs. 3 and 4 we present measured and calculated BLS spectra for the Rayleigh mode of a Si(001) wafer for $\theta_i = 30^\circ$ and 70° , respectively. The sample was oriented so that the [110] direction was along the β axis. Our spectrometer is a tandem six-pass Fabry-Perot interferometer for which the mirror separation was 5 mm, corresponding to a free spectral range (FSR) of 30 GHz. Light from a single-longitudinal mode Ar⁺ laser ($\lambda = 514.5$ nm), polarized in the y - z plane (p polarized) was incident on the sample, and both p - and s -polarized scattered light were collected. The spectra marked No Slit in Figs. 3 and 4 were collected with a circular aperture corresponding to a lens f -number of $f/2$. For the No Slit spectrum shown in Fig. 3, the feature is really a single peak. However, the small right-angle prism used to guide the incident light (Fig. 1) and its supporting rod block the central part of the aperture. For small values of θ_i , this causes a small dip within the broad peak, as has been reported by Karanikas *et al.*¹⁶ who used the frequency corresponding to the dip minimum as a measure of the peak position. The dip in the central part of the peak is not observed on the $\theta_i = 70^\circ$ spectrum because for large θ_i the aperture-broadening effect is smaller and the dip is smeared out by the convolution of the aperture-broadened spectrum with the spectrometer instrumental function, which has a

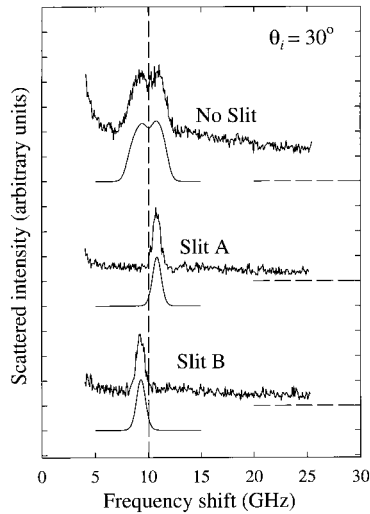


Fig. 3. Measured and calculated spectra for the Rayleigh mode of Si(001). For the measured peaks: $\theta_i = 30^\circ$, lens $f/2$, [110] direction of sample along β direction, FSR = 30 GHz. Calculated curves: $v_R = 5080$ m/s,¹⁴ $\epsilon = 17.8 + 0.506i$.¹⁵ The vertical dashed line represents the position of the peak for an infinitesimal lens aperture and the horizontal dashed lines represent zero-scattered intensity for each spectrum. Collection times are 2.76, 1.69, and 1.48 s/data point for the No Slit, Slit A, and Slit B spectra, respectively.

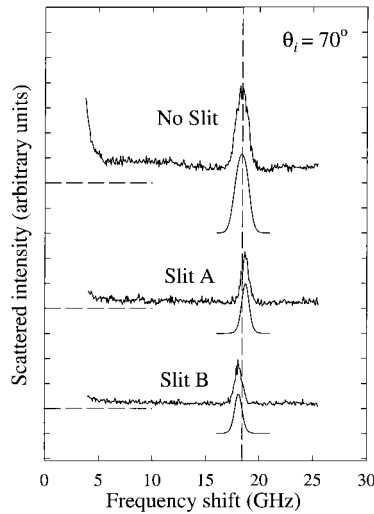


Fig. 4. Same as Fig. 3, but for $\theta_i = 70^\circ$. Collection times are 1.25, 1.23, and 1.35 s/data point for the No Slit, Slit A, and Slit B spectra, respectively.

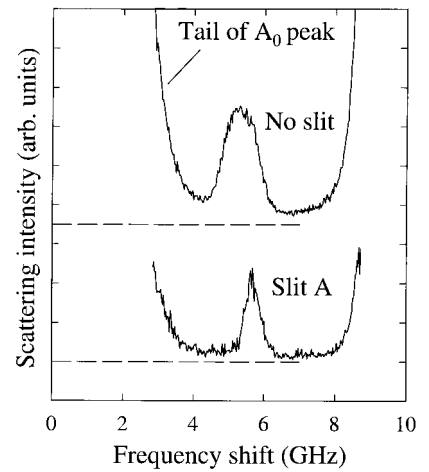


Fig. 5. BLS spectra for a freely standing polystyrene film, 75 nm thick, $\theta_i = 45^\circ$, FSR = 10 GHz, and $f/2$ lens. The instrumental FWHM was 0.4 GHz. The horizontal dashed lines represent zero-scattered intensity for each spectrum. Collection times are 4.38 and 1.68 s/data point for the No slit and Slit A spectra, respectively.

linewidth of approximately 0.80 GHz FWHM typically for a FSR of 30 GHz. Spectra collected with a slit to accept a selected part of the total lens aperture are also presented in Figs. 3 and 4. In Figs. 2(a) and 2(b) are shown the two locations of the slit that have been used in the measurements, relative to the aperture of the collecting lens. In terms of the (α, β) coordinates of Figs. 2(a) and 2(b), the slits are centered at $\beta = -0.085$ (slit A) and $+0.085$ (slit B), and are 0.067 wide.

In Figs. 3 and 4 we also show line shapes that are calculated with the method presented above, corresponding to each of the experimental spectra. Each calculated curve is the convolution of the aperture-broadened line shape with the instrumental function that was determined directly from the corresponding experimental spectrum. The vertical dashed line in the Figs. 3 and 4 represent the position of the peaks in the case of an aperture with infinitesimal diameter and the horizontal dashed lines represent zero-scattered intensity for each of the spectra. One can see that the broadening that is due to the collecting aperture is in general complicated. For large angles of incidence, the asymmetry of the broadening results in peak positions that are downshifted with respect to the position of the dashed line, e.g., a shift of approximately 2% is obtained for $\theta_i = 70^\circ$. This effect was also discussed briefly in Ref. 13 in terms of the dependence of the scattering cross section on the direction of \mathbf{k}^i and \mathbf{k}^s . Both this and the distribution of

wave-vector magnitudes in the collecting lens aperture lead to a downshift of the peak position.

In Tables 1 and 2 the measured and calculated FWHM values are listed for the spectra of Figs. 3 and 4. The last column of each table gives the instrumental linewidths determined from the unshifted laser line for each spectrum, which have been used in the convolution to obtain the calculated spectra. All linewidths of a particular row should be compared with their respective instrumental linewidth. Slit A, in the negative β region, gives slightly better results for the $\theta_i = 30^\circ$ spectrum. A narrower slit can be used, at the expense of a longer collection time. For wider slits and/or smaller spectrometer linewidths, the effect of the position of the slit is more significant. Results shown in Tables 1 and 2 validate the assumption that the Rayleigh mode of Si(001) has a natural linewidth that is small compared with the instrumental linewidth. The small discrepancies between measured and calculated FWHM's are likely due to the limited statistics of the collected spectra, as

Table 1. Measured and Calculated Peak Frequency and FWHM of Phonon Peaks Presented in Fig. 3 ($\theta_i = 30^\circ$)

Curve	Measured	Measured	Instrumental	Instrumental
	Frequency	Frequency		
	(GHz)	(GHz)	(GHz)	(GHz)
	$\pm 1\%$	$\pm 3\%$	$\pm 2\%$	
No slit	10.0 ^a	10.0 ^a	3.5	0.87
Slit A	10.8	10.65	0.83	0.80
Slit B	9.3	9.15	0.91	0.82

^aFrequency of dip in measured peak.

Table 2. Measured and Calculated Peak Frequency and FWHM of Phonon Peaks Presented in Fig. 4 ($\theta_i = 70^\circ$)

Curve	Measured		Measured		Instrumental FWHM (GHz) $\pm 2\%$
	Frequency (GHz) $\pm 1\%$	Frequency (GHz)	FWHM (GHz) $\pm 3\%$	FWHM (GHz)	
No slit	18.3	18.38	1.24	1.36	0.83
Slit A	18.6	18.78	0.82	0.80	0.79
Slit B	18.1	18.18	0.81	0.83	0.80

can be inferred from the small variations in instrumental FWHM from spectrum to spectrum.

Aperture broadening as well as frequency shift is directly proportional to the phonon sound velocity and is significant only if it is larger than the instrumental linewidth. For the Fabry–Perot interferometer used in BLS, the instrumental linewidth is proportional to the FSR. Therefore there will be broadening even if the sound velocity is small because of the necessity of scanning over a smaller range of frequencies. In Fig. 5 we show SBLS spectra collected for a freely standing polystyrene film (transparent material, real index of refraction $n = 1.59$) that is 75 nm thick, suspended across a 3-mm-diameter aperture. For measurements of the film properties as a function of film thickness and temperature,⁹ it is important to obtain precise values for the phonon frequencies and linewidths. The peak in the spectra of Fig. 5 is the first symmetric plate mode (S_0)¹⁷ with a sound velocity of approximately 1800 m/s. The lowest-order asymmetric mode (A_0) has a frequency that is too small to be resolved from the unshifted laser line. The angle of incidence was $\theta_i = 45^\circ$ and the FSR was 10 GHz, with an instrumental FWHM of 0.4 GHz. One can see that use of the slit decreases the FWHM of the measured peak to a value comparable with the instrumental FWHM, thereby showing that the phonon natural linewidth is smaller than 0.4 GHz.

5. Conclusions

In SBLS measurements, aperture broadening of the phonon peaks is generally significant. At small angles of incidence, the broadening is large (as much as 60% of the peak frequency shift) and asymmetric. At large angles of incidence, the broadening is smaller but asymmetric, and the broadened peak is downshifted in frequency compared with the unbroadened peak. By calculating the SBLS line shape for the fundamental surface acoustic wave, the Rayleigh mode, accounting for the spread in the scattering wave vectors across the collecting lens aperture, the polarization and angular dependence of the scattering, and the spectrometer instrumental function, we obtained a detailed comparison between measured and calculated Rayleigh-mode line shapes for SBLS from Si(001). We demonstrated that the placement of a rectangular slit in the collected scattered light is an effective method to reduce line broadening

that is due to aperture effects without producing significant reductions in the peak intensity.

The authors thank J. A. Forrest for collecting the polystyrene film spectra, and S. Lee and B. Hillebrands for useful discussions. This research was funded by the Natural Sciences and Engineering Research Council of Canada.

References

1. H. Z. Cummins, "Brillouin scattering studies of phase transitions in crystals," in *Light Scattering Near Phase Transitions*, H. Z. Cummins and A. P. Levanyuk, eds. (North-Holland, Amsterdam, 1983), pp. 359–447.
2. H. Z. Cummins, G. Li, W. M. Du, J. Hernandez, and N. J. Tao, "Light scattering spectroscopy of the liquid-glass transition," *J. Phys.: Condens. Matter* **6**, A51–A62 (1994).
3. J. R. Sandercock, "Trends in Brillouin light scattering: studies of opaque materials, supported films and central modes," in *Light Scattering in Solids III*, M. Cardona and G. Güntherodt, eds. (Springer-Verlag, Berlin, 1982), pp. 173–206.
4. J. R. Sandercock and W. Wettleing, "Light scattering from surface and bulk thermal magnons in iron and nickel," *J. Appl. Phys.* **50**, 7784–7789 (1979).
5. W. F. Oliver, C. A. Herbst, S. M. Lindsay, and G. H. Wolf, "A general method for determination of Brillouin linewidths by correction for instrumental effects and aperture broadening: application to high-pressure diamond anvil cell experiments," *Rev. Sci. Instrum.* **63**, 1884–1895 (1992).
6. H. G. Danielmeyer, "Aperture corrections for sound-absorption measurements with light scattering," *J. Acoust. Soc. Am.* **47**, 151–154 (1969).
7. S. Lee, "Elastic properties of polymeric Langmuir-Blodgett studied using Brillouin light scattering," Ph.D. dissertation (University of Arizona, Tucson, Ariz., 1991).
8. J. R. Dutcher, S. Lee, B. Hillebrands, G. J. McLaughlin, B. G. Nickel, and G. I. Stegeman, "Surface-grating-induced zone folding and hybridization of surface acoustic modes," *Phys. Rev. Lett.* **68**, 2464–2467 (1992).
9. J. A. Forrest, K. Dalnoki-Veress, J. R. Stevens, and J. R. Dutcher, "Effect of free surfaces on the glass transition temperature of thin polymer films," *Phys. Rev. Lett.* **77**, 2002–2005 (1996).
10. P. Mutti, C. E. Bottani, G. Ghislotti, M. Beghi, G. A. D. Briggs, and J. R. Sandercock, "Surface Brillouin scattering-extending surface wave measurements to 20 GHz," in *Advances in Acoustic Microscopy I*, G. A. D. Briggs, eds. (Plenum, New York, 1995), pp. 249–300.
11. L. Giovannini, F. Nizzoli, and A. M. Marvin, "Theory of surface acoustic phonon normal modes and light scattering cross section in a periodically corrugated surface," *Phys. Rev. Lett.* **69**, 1572–1575 (1992).
12. G. S. Agarwal, "Interaction of electromagnetic waves at rough dielectric surfaces," *Phys. Rev. B* **15**, 2371–2383 (1977).
13. R. Loudon and J. R. Sandercock, "Analysis of the light-scattering cross-section for surface ripples on solids," *J. Phys. C* **13**, 2609–2622 (1980).
14. G. W. Farnell, "Properties of elastic surface waves," in *Physical Acoustics, Principles and Methods*, W. P. Mason and R. N. Thurston, eds. (Academic, New York, 1970), Vol. 6, pp. 109–166.
15. E. D. Palik, ed., *Handbook of Optical Constants of Solids*, (Academic, New York, 1985), Vol. 1, p. 564.
16. J. M. Karanikas, S. Sooryakumar, and J. M. Phillips, "Dispersion of elastic waves in supported CaF_2 films," *J. Appl. Phys.* **65**, 3407–3410 (1989).
17. G. W. Farnell and E. L. Adler, "Elastic wave propagation in thin layers," in *Physical Acoustics, Principles and Methods*, W. P. Mason and R. N. Thurston, eds. (Academic, New York, 1972), Vol. IX, pp. 35–127.